Struct Multidisc Optim (2009) 37:305–318
DOI 10.1007/s00158-008-0233-8

RESEARCH PAPER

Optimal design of adaptive structures: Part I. Remodeling for impact reception

Marcin Wiklo · Jan Holnicki-Szulc

Received: 3 August 2007 / Revised: 18 October 2007 / Accepted: 18 December 2007 / Published online: 14 March 2008

Abstract The paper (written in two parts) is devoted to the presentation of numerical tools, based on the so-called *virtual distortion method* (VDM) for fast structural reanalysis and to the application of this tools for optimal design of adaptive structures exposed to impact loads. The first paper deals with fast modifications of the material distribution (coupled stiffness and mass redistribution) in dynamically loaded structures, which allows their optimal remodeling, e.g., to minimize average deflections. The VDM-based approach allows analytical sensitivity determination, which is very helpful in efficient implementation of the optimization procedure, utilized to solve the defined remodeling problem. The presented methodology is illustrated with a numerical example of truss–beam structure exposed to random impact loads.

Keywords Fast structural reanalysis · Virtual distortion method · Adaptive impact absorption · Optimal design · Impact loads

M. Wiklo (✉)
Institute of Applied Mechanics,
Technical University of Radom,
Radom, Poland
e-mail: mwiklo@ippt.gov.pl, marcin.wiklo@pr.random.pl

M. Wiklo · J. Holnicki-Szulc
Institute of Fundamental Technological Research,
Smart-Technology Centre,
Warsaw, Poland

J. Holnicki-Szulc
e-mail: holnicki@ippt.gov.pl

1 Nomenclature

AIA	adaptive impact absorbtion
VDM	virtual distortion method
IVDM	impulse virtual distortion method
IVFM	impulse virtual force method

2 Introduction

Structural design for dynamic loads is still a challenge, especially, in the case of unpredictable impact loads that demand for a very fast dynamic analysis modeling real structural response.

One can find very good numerical tools available commercially, capable of reliable simulation of structural response to the determined impact scenario. The majority of these programs are devoted to *crashworthiness* analysis for car collisions. Nevertheless, these tools are not very helpful when searching for the best design in the case of unknown a priori impact scenario. The trial-and-error approach seems to be the unique option in this case.

On the other hand, the so-called *smart technologies* have been developing fast over the last decade, giving hope for more sophisticated solutions, taking advantage from real-time impact load identification (cf. Sekua et al. 2006) and *plastic-like adaptation* of predesigned active elements (so-called *structural fuses*) to the actual impact loads (cf. Holnicki and Knap 2004).

The main motivation for writing this paper is to propose a methodology for optimal design of such *adaptive structures* for *adaptive impact absorption* (AIA). The first part is devoted to the remodeling (material redistribution) of elastic structures exposed to impact

loads, while the second one extends the optimization on adaptive structures, equipped with controllable structural fuses able to mimic a plastic-like behavior.

From the time when the idea of optimal structural remodeling (including topological optimization) has been presented (Kikuchi and Bendse 1992) as a problem of material distribution, the subject has been continuously developed for more and more complex structures, taking nonlinear behavior into account as well, including the impact resistance design of vehicles. The formulation of the problem for many loading states was presented in Diaz and Bendse (1992). A minimization of the maximal compliance for many load states can be achieved with the application of the β method Bendsoe and Taylor (1984), Tvergaard (1975) or the Kreisselmeier–Steinhauser function method Steinhauser and Kreisselmeier (1979). In the analysis of impact resistance of vehicles, we can expect a long list of specific problems: nonlinear materials (plasticity, hardening), nonlinear geometry (large displacements, deformations, buckling), dynamics, or contact. The first papers addressing design for impact resistance are Mayer et al. (1996), Kikuchi et al. (1998), Maute et al. (1998), Marzec and Holnicki-Szulc (1999), Holnicki-Szulc and Knap (1999), and Diaz and Soto (1999).

The design of complex and complicated structures, such as structures of automobiles, is an iterative process due to safety aspects. First, design changes are performed, and then, the structure undergoes simulation once more. A duration of a single analysis of the whole structure can take many hours (24–30 h with the application of supercomputers, whereas it takes several days when work stations are used), according to the 2002 data Soto (2002). An evaluation of influence of each modification requires a renewed analysis of the system. Manual change of parameters and application of a precise model make the simulation process tedious, not effective, numerically expensive, and time consuming. Therefore, in the early stage of design and redesign, it is recommended to use simplified models which are numerically less expensive and which allow to automatize the remodeling process.

For linear systems, the technique of simplified processes has been developed and applied for many years, while for nonlinear systems, especially those which were subjected to a dynamical loading, there were few papers published until now. Models with concentrated mass in analysis and design of structures have been used in the automobile industry for safety improvement during crash tests since the early 1970s Kamal (1970); Kamal and Wolf (1982). In these models, nonstructural elements were modeled with concentrated masses, whereas structural elements, which underwent the deformation, were modeled as nonlinear spring elements. The load–displacement characteristic was the same as the characteristic generated for crashed tubes. Models with concentrated masses were applied to the passenger–automobile dynamical simulation Wang et al. (1991). In Song and Ni (1986), three simulation methods (hybrid method, analytical method, and mixed method) of automobile structures exposed to impact were presented with examples. In these methods, the structural elements were modeled with nonlinear spring elements. Their load–displacement characteristic was generated during laboratory tests. El-Bkaily et al. (1993) describes in detail a fast method of simulation and design of automobile structure frames, called V-CRASH method. More information about the development of simplified models can be found in Mijar et al. (1999) and Kim et al. (2001). An indispensable stage of application of rough models is the identification of the model. The subject was developed in many works for different structures (for instance: nuclear reactors, buildings exposed to earthquakes, and other problems of civil engineering). The impact resistance of automobile vehicles was also considered in other papers, e.g., in Pedersen (2002a, b, c), Ignatovich and Diaz (2002), Ignatovich et al. (2000).

The *virtual distortion method* (VDM) is a robust and versatile numerical tool for fast and exact structural modifications (Kolakowski et al. 2007) which is able to introduce material redistribution (including vanishing of structural elements) and piecewise-linear nonlinearity into constitutive lows. It is also capable of exact (analytical) sensitivity analysis and effective, gradient-based optimal redesign algorithms, without need for modifications of the global stiffness and mass matrices.

The present state of the VDM method development includes dynamic problems mentioned above. However, the coupled problem of structural modification (material redistribution in elasto-plastic structures causing interacting modifications of mass, stiffness, and plastic zone distribution) and its sensitivity analysis is still unsolved. Therefore, the following problems of fast re-analysis with the VDM method are still a research challenge:

- Modeling coupled modifications (simultaneous modifications of mass, stiffness, and physical nonlinearities)
- Sensitivity analysis of dynamic responses due to coupled structural modifications.

The first objective of this paper is to contribute to the aforementioned research problems, elaboration of related algorithms, as well as their implementation via

the generalized VDM method. This will require introduction of *virtual forces* modeling modifications of mass distribution as well as *virtual distortions* modeling stiffness modifications of structural elements. In the coupled problems, a superposition of these two distortion fields will be applied. The third field of virtual distortions modeling physical nonlinearities will be also taken into account to simulate plastic-like response of adaptive structures.

The second objective of this paper is to demonstrate the effectiveness of the newly created numerical tools for solving nonstandard engineering problems such as optimal design of adaptive structures to increase their capacity of impact load absorption (AIA problem).

The problem of redesigning AIA structures with controllable plastic thresholds triggering the yielding of active elements (in dependence on the identified 'online' impact) to increase the impact absorption effectiveness has not been analyzed in scientific literature so far. A generalized VDM method allows for the description and solution of the problem with a gradient-based optimization approach. A necessity to restrict considerations to small deformations and to approximate physical relations by piecewise linear characteristics causes an error of the simulated dynamic response increasing with time. However, it gives a chance for creation of an effective tool, which allows determining the material redistribution in the initial phase of dynamic response, while the structure deformations are still below an arbitrary assumed value. When material redistribution is completed, a precise numerical simulation of the dynamical structural response (with large deformations) can be performed with one of the commercially available codes. The simplest truss model of a structure was chosen due to simplicity of considerations, which does not reduce the generality of the proposed approach, applicable to other types of structures, for example, frame or plate structures (Holnicki-Szulc and Gierlinski 1995). However, the generalized approach to the mentioned types of structures requires introduction of more developed distortion states, able to model potential modifications of the structure.

The paper includes:

- Presentation of methodology for fast coupled modifications (stiffness and mass modification due to material redistribution) of elasto-plastic structures imposed to dynamical loading,
- Corresponding analytical sensitivity analysis,
- Structural optimization (remodeling) due to maximization of the overall structural stiffness under one or more impact loading states (part I of the paper), and
- Optimal adaptation of the AIA structure with a given geometry (determined in the I part of the paper) for real-time identified impact to maximize the impact energy dissipation (the II part of the work).

3 Modeling of structural modifications via virtual distortions and forces

This part presents a methodology and a corresponding numerical tool for fast and precise reanalysis of structures imposed to dynamical loading, allowing effective modification in the optimal remodeling process. Combined modifications of cross-sectional areas (A), element stiffnesses (E), and masses (M) corresponding to material redistribution in the process of structural optimal remodeling will be discussed.

In the whole paper, lower case subindices refer to elements, while capital subindices refer to nodes in the global coordinate systems. Einstein's summation rule is used; underlined indices are exempt of summation.

3.1 Methods based on influence matrices

Besides a short description of the *impulse virtual distortion method* (IVDM) generalizing the classical VDM method on dynamic problems (Zieliski 2004), applicable in modeling of stiffness redistribution, the so-called *impulse virtual forces method* (IVFM) will be proposed to model mass redistributions. A combination of these two methods gives a basis for creation of the complete numerical tool for the simulation of structural remodeling.

Let us assume the following terminology:

Modified structure	Structure in which some parameters (stiffness, mass, etc.) have been modified
Modeled structure	Structure with an originally defined configuration (stiffness and mass matrices) and modifications being modeled with virtual methods

The VDMs allow the determination of the modified structure response by using the so-called *influence matrices* determined for the original structure. The response of the modified structure is being determined without a need to renew the analysis of the whole structure with modifications.

Let us demonstrate the IVDM method using the example of the truss structure (cf. testing example, Kolakowski et al. 2007) with the initial distribution of structure parameters and the dynamic response $\varepsilon^L(t)$.

To determine how local modifications applied in selected elements affect the entire structure (local–global interactions), a selected element was subjected to a unitary impulse elongation applied in the time instance t (*virtual distortion*, $\varepsilon^0(t)$), which can be physically interpreted, e.g., as thermal impulse applied to the rod. The compatible strains $\varepsilon^R(t)$ were generated in the structure as the response. In general, the following formula can be used to describe residual strains (related to the corresponding self-equilibrated stresses) caused by an arbitrary selected virtual distortion scenario:

$$\varepsilon_i^R(t) = \sum_{\tau \le t} D_{ij}^{\varepsilon}(t-\tau)\,\varepsilon_j^0(\tau) \tag{1}$$

where $D_{ij}^{\varepsilon}(t-\tau)$ denotes a dynamic *influence matrix* containing strains $\varepsilon(t)$ induced in structural elements as the response to the unitary virtual distortion impulse $\varepsilon_j^0(\tau)$ applied in selected elements in the time instance τ. The impulse is applied as a Dirac-like function in the form of a pair of balanced forces causing unitary deformation. Assuming geometrical linearity, the principle of super-position can be applied. The response of the modeled structure can be expressed as a sum of the linear response $\varepsilon^L(t)$ and the component $\varepsilon^R(t)$ modeling modifications via virtual distortions (Fig. 1).

$$\varepsilon_i(t) = \varepsilon_i^L(t) + \sum_{\tau \le t} D_{ij}^{\varepsilon}(t-\tau)\varepsilon_j^0(\tau). \tag{2}$$

The above IVDM method allows to model modifications of the structural stiffness distribution. However, to model mass redistribution, the modified approach IVFM is proposed. The IVFM implementation is analogous to the previously described approach. First step is to determine displacements of the unmodified structure $u^L(t)$. Then, the unitary forces $F(t) = 1 \cdot \delta$ are applied to particular degrees of freedom related to modified elements to generate the dynamic influence matrix

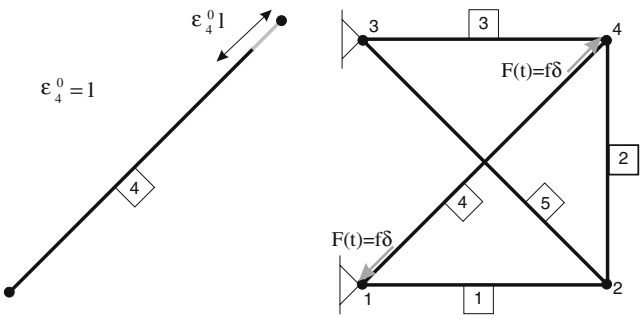

Fig. 1 Unitary virtual distortion

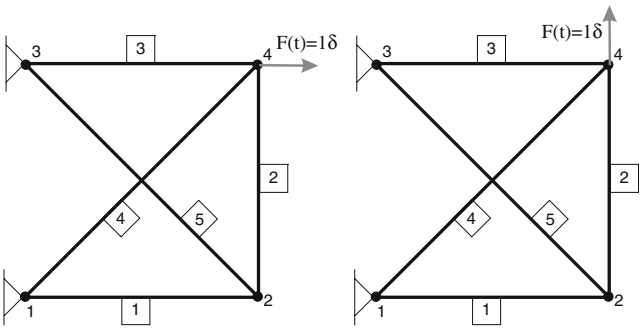

Fig. 2 Unitary virtual forces

(Fig. 2). Application of the virtual force impulses generates a time variable field of displacements $u^R(t)$:

$$u_N^R(t) = \sum_{\tau \le t} B_{NM}^{p}(t-\tau)\,p_M^0(\tau) \tag{3}$$

where $B_{MN}^{p}(t-\tau)$ is a dynamical *influence matrix*.

Assuming geometrical linearity, the modeled structure response can be expressed as a sum of the linear responses $u^L(t)$ and the component $u^R(t)$ modeling modifications via virtual forces (Fig. 2)

$$u_N(t) = u_N^L(t) + \sum_{\tau \le t} B_{NM}^{p}(t-\tau)\,p_M^0(\tau). \tag{4}$$

3.2 Modifications of stiffness and mass distribution (parameters E and M)

The summation over time in the previous section indicates the discretization of the analyzed period of time $\langle 0, 1, \ldots, t, \ldots, T\rangle$. For performing time integration, the authors chose the Newmark integration scheme. Except for the initial condition $t = 0$, all other quantities are calculated starting from the first time step onward. Therefore, to be consistent with the numerical integration procedure, the calculation of strains in the *modeled* structure should be formally modified [cf. (2)]:

$$\varepsilon_i(t) = \varepsilon_i^L(t) + \sum_{\tau \le t} D_{ij}^{\varepsilon}(t+1-\tau)\varepsilon_j^0(\tau) \tag{5}$$

where the vector component $\varepsilon_i^L(t)$ denotes the development of strains in the i-th element of the structure, determined for the elastic structure with initial redistribution of stiffnesses. $D_{ij}^{\varepsilon}(t+1-\tau)$ is a dynamic *influence matrix* which describes the evolution of strains in the i-th element in the t-th time moment due to a unitary impulse of virtual distortion generated in the τ-th time moment within the j-th element.

The corresponding stresses induced in the structure take the form:

$$\sigma_i(t) = E_{\underline{i}}\left(\varepsilon_{\underline{i}}(t) - \varepsilon^0_{\underline{i}}(t)\right)$$

$$\sigma_i(t) = \sigma_i^L(t) + E_{\underline{i}}\left[\sum_{\tau<t} D^{\varepsilon}_{\underline{i}\,j}(t+1-\tau)\varepsilon^0_j(\tau) + \left(D^{\varepsilon}_{\underline{i}\,j}(1) - \delta_{\underline{i}\,j}\right)\varepsilon^0_j(t)\right] \tag{6}$$

where $\sigma_i^L(t)$ describes the development of stresses for the initial structure configuration.

To determine the *virtual distortion* development $\varepsilon^0(t)$ simulating stiffness modifications, equality of forces p and deformations $\varepsilon(t)$ in the *modified* and *modeled* structures has to be postulated:

$$\hat{p}_i(t) = \hat{E}_{\underline{i}} A_{\underline{i}} \varepsilon_{\underline{i}}(t) \tag{7}$$

$$p_i(t) = E_{\underline{i}} A_{\underline{i}}\left(\varepsilon_{\underline{i}}(t) - \varepsilon^0_{\underline{i}}(t)\right). \tag{8}$$

In the consequence, the following formulas allowing determination of $\varepsilon^0(t)$ can be delivered:

$$\varepsilon^0_i(t) = (1-\mu^{\mathrm{E}}_{\underline{i}})\varepsilon_{\underline{i}}(t)$$

$$\left[\delta_{ij} - (1-\mu_{\underline{i}})B^{\varepsilon}_{\underline{i}j}(1)\right]\varepsilon^0_j(t) = (1-\mu^E_{\underline{i}})\varepsilon^{\neq t}_{\underline{i}}(t) \tag{9}$$

where $\varepsilon_i^{\neq t}$ denotes strains in the element i with influence of *virtual distortion* $\varepsilon^0_j(t)$ in the time step t not taken into account:

$$\varepsilon^{\neq t}_i(t) = \varepsilon^L_i(t) + \sum_{\tau=1}^{t-1} B^{\varepsilon}_{ij}(t+1-\tau)\varepsilon^0_j(\tau) \tag{10}$$

whereas μ_i^E is a parameter of the local stiffness modification and it is expressed by the following relation:

$$\mu^{\mathrm{E}}_i \overset{\mathrm{def}}{=} \frac{\hat{E}_{\underline{i}}}{E_{\underline{i}}} = \frac{\varepsilon_{\underline{i}}(t) - \varepsilon^0_{\underline{i}}(t)}{\varepsilon_{\underline{i}}(t)}. \tag{11}$$

The modification parameter determines a ratio of the new (modified) stiffness $\hat{E}$ to the original one E. The parameter $\mu^E \in \langle 0, \mu^{E\max}\rangle$ should be interpreted as following: For $\mu = 0$, the element stiffness disappears; for $\mu = 1$, there is no stiffness modification in the element, whereas for $\mu = \mu^{\mathrm{E}\max}$, the maximal acceptable modification of the element stiffness is obtained.

The equations of motion for the structure with *modified* mass matrix and for the *modeled* structure with virtual force simulating this modification can be described in the form:

$$\hat{M}_{NM}\ddot{u}_M(t) + K_{NM}u_M(t) = f_N(t) \tag{12}$$

$$M_{NM}\ddot{u}_M(t) + K_{NM}u_M(t) = f_N(t) + p^0_N(t) \tag{13}$$

where $\hat{M}_{NM}$ denotes the mass matrix being modified by change of material density, whereas $p^0_N(t)$ is a vector of virtual forces responsible for modeling of mass modification.

To determine the virtual force development $\mathbf{p}^0(t)$ simulating the mass redistribution, the equivalence between inertia forces of the *modeled* structure (13) and the *modified* one (12) should be postulated:

$$\hat{M}_{NM}\ddot{u}_M = M_{NM}\ddot{u}_M - p^0_N(t) \tag{14}$$

which leads to the conclusion:

$$p^0_N(t) = -\Delta M_{NM}\ddot{u}_M(t) \tag{15}$$

where:

$$\Delta M_{NM} = \sum_i \left(\mu^{\mathrm{A}}_{\underline{i}} - 1\right) A_{\underline{i}}\rho_{\underline{i}}l_{\underline{i}}\, \overset{i}{a}_{Nr} M^{el}_{rs}\, \overset{i}{a}_{sM} \tag{16}$$

ρ_i is the element's density, l_i denotes the length of a structural element i, a_{Nr} matrix defines a local–global transformation, and M^{el}_{rs} is the element consistent mass matrix. The coefficient μ_i^{A} defines the ratio of modified density to the original one (or the modified cross-sectional area to the original one):

$$\mu^{\mathrm{A}}_i \overset{\mathrm{def}}{=} \frac{\hat{A}_i}{A_i} = \frac{\hat{\rho}_i}{\rho_i} \overset{\mathrm{def}}{=} \mu^{\mathrm{R}}_i \tag{17}$$

The dynamic structural response is determined by IVFM as a superposition of virtual fields and initial response as follows:

$$u_N(t) = u^L_N(t) + \sum_{\tau\le t} B^p_{NM}(t+1-\tau)p^0_M(\tau) \tag{18}$$

where the vector of virtual forces $p^0_M(t)$ simulates mass modifications, whereas the $u^L_N(t)$ vector denotes the development of displacements for the initial elastic structure; $B^p_{NM}(t+1-\tau)$ is the dynamical *influence matrix*. The$N$ indices refer to all degrees of freedom of the system, whereas the M indices refer to degrees of freedom for modified elements.

The nodal accelerations [necessary in the calculation of the virtual forces $\mathbf{p}^0(t)$] are being determined for all time steps from the following relations:

$$\ddot{u}_N(t) = \ddot{u}_N^L(t) + \sum_{\tau \le t} \ddot{B}^p_{NM}(t+1-\tau)\, p^0_M(\tau) \tag{19}$$

where $\ddot{u}_N^L(t)$ is the vector which describes accelerations of the unmodified structure. $\ddot{B}^p_{NM}(t+1-\tau)$ is the dynamic *influence matrix*. It describes the history of accelerations for corresponding degrees of freedom, due to unitary force impulses applied in degrees of freedom related to locations of modification.

The equation, from which virtual forces are determined, is obtained by substituting the accelerations (19) into the virtual force relation (15):

$$\left[\delta_{NM} + \Delta M_{NM} \ddot{B}^p_{NM}(1)\right] p^0_M(t) = -\Delta M_{NM} \ddot{u}^{\neq t}_M(t) \tag{20}$$

where the $\ddot{u}^{\neq t}_M(t)$ is an acceleration vector in which influences of virtual forces $p^0_M(t)$ at the actual time step t were not taken into account:

$$\ddot{u}^{\neq t}_N(t) = \ddot{u}^L_N(t) + \sum_{\tau=1}^{t-1} \ddot{B}^p_{NM}(t+1-\tau)\, p^0_M(\tau). \tag{21}$$

3.3 Modifications of material distribution (coupling parameter A)

The structural modifications described in the previous section refer, e.g., to changes of the structural material in selected elements, causing modifications of material density and/or modification of the element mass. The formulas (9) and (20) allow in this case the determination of virtual components (virtual distortions and/or forces) simulating the structural modifications.

The modification of cross-sectional areas A is related not only to stiffness matrix $\mathbf{K}$ modifications but also to the modification of the mass matrix $\mathbf{M}$. The equation of motion for the system with *modified* cross-section areas $\hat{A}$ (modified mass $\hat{\mathbf{M}}$ matrix as well as stiffness matrix $\hat{\mathbf{K}}$) can be written as follows:

$$\hat{M}_{NM}\ddot{u}_M(t) + G^T_{Ni}\hat{S}_{ij}G_{jM}u_M(t) = f_N(t). \tag{22}$$

On the other hand, (22) formulated for the *modeled* can be written using virtual forces $p^0(t)$ simulating mass modifications and virtual distortions $\varepsilon^0(t)$ simulating stiffness modifications in the following manner:

$$M_{NM}\ddot{u}_M(t) + G^T_{Ni}S_{ij}\left[G_{jM}u_M(t) - l_{\underline{j}}\varepsilon^0_{\underline{j}}(t)\right] = f_N(t) + p^0_N(t) \tag{23}$$

where $\hat{S}_{ij}$ and S_{ij} are diagonal matrices with elements over diagonal $\hat{S}_{ii} = E_{\underline{i}}\hat{A}_{\underline{i}}/l_{\underline{i}}$ and $S_{ii} = E_{\underline{i}}A_{\underline{i}}/l_{\underline{i}}$, respectively, E_i denoting Young's modulus, A_i cross-sectional area, and l_i the length of an element i. The matrix G_Ni is a transformation matrix, whose elements are related to cosines of angles between elements and directions of degrees of freedom. Equation (23) can be also written applying the strain vector as:

$$M_{NM}\ddot{u}_M(t) + G^T_{Ni}S_{ij}\left[l_{\underline{j}}\left(\varepsilon_{\underline{j}}(t) - \varepsilon^0_{\underline{j}}(t)\right)\right] = f_N(t) + p^0_N(t). \tag{24}$$

The dynamic structural response is determined as a superposition of the response of a structure with unmodified cross-sections and the response due to virtual fields simulating modifications (ε^0, responsible for the stiffness remodeling and p^0, responsible for mass remodeling) in the following way:

$$u_N(t) = u^L_N(t) + \sum_{\tau \le t} B^{\varepsilon}_{Nj}(t+1-\tau)\varepsilon^0_j(\tau) + \sum_{\tau \le t} B^p_{NM}(t+1-\tau)\, p^0_M(\tau) \tag{25}$$

where the N index addresses all degrees of freedom of the system, the j refers to all elements with cross-sectional area modifications, while M refers to all degrees of freedom related to modified element cross-sections.

The strain vector $\varepsilon(t)$ can be obtained by multiplying (25) by the $\frac{1}{L_{\underline{i}}}G_{\underline{i}N}$ value:

$$\varepsilon_i(t) = \varepsilon^L_i(t) + \sum_{\tau \le t} D^{\varepsilon}_{ij}(t+1-\tau)\varepsilon^0_j(\tau) + \sum_{\tau \le t} D^p_{iM}(t+1-\tau)\, p^0_M(\tau). \tag{26}$$

Expressing forces in the *modified* (27) and *modeled* (8) structure by

$$\hat{p}_i(t) = E_{\underline{i}}\hat{A}_{\underline{i}}\varepsilon_{\underline{i}}(t) \tag{27}$$

and postulating identity of forces and strains for both structures, the identity of right hand side expressions

from (8) and (27) can be obtained. Taking into account the modification parameters related to changes of cross-sectional areas (cf. (11)):

$$\mu_i^{\mathrm{A}} \stackrel{\mathrm{def}}{=} \frac{\hat{A}_{\underline{i}}}{A_{\underline{i}}} = \frac{\varepsilon_{\underline{i}}(t) - \varepsilon_{\underline{i}}^0(t)}{\varepsilon_{\underline{i}}(t)} \tag{28}$$

and making use of the strain expression (26), the postulated condition can be expressed as follows:

$$\left[\delta_{ij} - (1-\mu_{\underline{i}}^{\mathrm{A}}) D_{\underline{i}j}^{\varepsilon}(1)\right] \varepsilon_j^0(t) - (1-\mu_{\underline{i}}^{\mathrm{A}}) D_{\underline{i}M}^{P}(1) p_M^0(t) = \left(1-\mu_{\underline{i}}^{A}\right) \varepsilon_{\underline{i}}^{\neq t}(t). \tag{29}$$

To obtain the second condition allowing (together with (29)) determination of the virtual components simulating combined modifications of mass and stiffness, equality of inertia forces of the *modified* structure and the *modeled* one should be also postulated (14), which leads to the definition of virtual forces $\mathbf{p}^0(t)$ (15). The matrix of mass increment $\Delta\mathbf{M}$ is already calculated (16), while the acceleration vector $\ddot{\mathbf{u}}(t)$ should be determined from the following relation:

$$\ddot{u}_N(t) = \ddot{u}_N^L(t) + \sum_{\tau \le t} \ddot{B}_{NM}^p(t+1-\tau) p_M^0(\tau) + \sum_{\tau \le t} \ddot{B}_{Nj}^{\varepsilon}(t+1-\tau) \varepsilon_j^0(\tau) \tag{30}$$

where the influence matrices $\ddot{B}(t)$ describe the history of accelerations resulting from unitary impulses of virtual force or distortion.

The second condition, essential in the determination of the virtual components, is being obtained by the substitution of (30) into (15):

$$\Delta M_{NM} \ddot{D}_{Mj}^{\varepsilon}(1) \varepsilon_j^0(t) + \left[\delta_{NK} + \Delta M_{NM} \ddot{D}_{MK}^{p}(1)\right] p_K^0(t) = -\Delta M_{NM} \ddot{u}_M^{\neq t}. \tag{31}$$

Finally, a set of equations for the determination of virtual distortions and forces, modeling modifications of the cross-sectional area and mass, respectively, is obtained and has the following form:

$$\begin{bmatrix} \left[\delta_{ij} - (1-\mu_{\underline{i}}^{\mathrm{A}}) D_{\underline{i}j}^{\varepsilon}(1)\right] & (1-\mu_{\underline{i}}^{\mathrm{A}}) D_{\underline{i}K}^{P}(1) \\ \Delta M_{NM} \ddot{B}_{Mj}^{\varepsilon}(1) & \left[\delta_{NM} + \Delta M_{NK} \ddot{B}_{KM}^{p}(1)\right] \end{bmatrix} \begin{bmatrix} \varepsilon_j^0(t) \\ p_M^0(t) \end{bmatrix} = \begin{bmatrix} \left(1-\mu_{\underline{i}}^{A}\right) \varepsilon_{\underline{i}}^{\neq t}(t) \\ -\Delta M_{NM} \ddot{u}_M^{\neq t} \end{bmatrix}. \tag{32}$$

The principal matrix of the above set of equations is time independent and needs to be determined only once. It is also indispensable during the sensitivity analysis. The short version of the above equation can be as follows:

$$\mathbf{F}\mathbf{d}^0 = \mathbf{b} \tag{33}$$

where $\mathbf{d}^0$ denotes the vector in which all virtual components are collected.

The algorithm for material redistribution analysis is shown in Fig. 3.

3.4 Numerical test

To present the correctness of the simulation process of structural modifications (with use of IVDM and IVFM), we will consider a truss cantilever structure shown in Fig. 4. The dynamic loading is realized by application of an initial velocity $V_0 = -20$ m/s to the second node in Fig. 4. Material properties are uniformly distributed; Young's modulus and density are $E = 210$ GPa and $\rho = 7{,}800$ kg/m^3, respectively. The cross-section of all elements is $A = 100$ mm^2, whereas dimensions of the structure are presented in the figure.

The results of structural modification (defined in Table 1) obtained via the VDM-based approach have been compared to a finite-element model (FEM)-based structural reanalysis performed for the remodeled structure. Considering the negligible deviations of the results obtained, for the purpose of comparison, an additional parameter, which characterizes a relative

Data and initial calculations
Input data:
- Construction under external load
- Determined modification parameters μ_i and initial values

Calculations:
- Linear construction response $\varepsilon^L(t), \ddot{u}^L$
- Dynamic influence matrices $\mathbf{D}, \ddot{\mathbf{B}}$
- Calculation of principal time independent matrix $\mathbf{F}$ for material distribution (32)

Calculation for each time increment t:
(a) Strains $\varepsilon^{\neq t}(t)$ and accelerations $\ddot{u}^{\neq t}$
(b) Calculate virtual components $\varepsilon^0(t)$, $p^0(t)$ (32)
(c) Update strain and accelerations according to calculated virtual parameters:
$\varepsilon_i(t) = \varepsilon_i^{\neq t}(t) + D_{ij}^{\varepsilon}(1)\varepsilon_j^0(t) + D_{iM}^{p}(1)p_M^{0A}(t)$
$\ddot{u}_i(t) = \ddot{u}_i^{\neq t}(t) + \ddot{B}_{ij}^{\varepsilon}(1)\varepsilon_j^0(t) + \ddot{B}_{iM}^{p}(1)p_M^{0A}(t)$
(d) If necessary calculate the gradient components
(e) If necessary calculate displacement $u(t)$, velocities $\dot{u}(t)$ and stresses $\sigma(t)$
(f) Go to (a)

Fig. 3 Algorithm for simulation of material redistribution

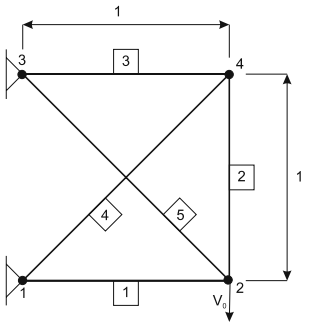

Fig. 4 The testing truss structure

difference between the results, was introduced based on the formula:

$$\Delta e_i(t) = \frac{e_i^R(t) - e_i^{IVDM}(t)}{e_i^R(t)} \tag{34}$$

where e is the determined value (strain, displacement, plastic distortion, etc.). The upper-scripts $()^R$ and $()^{\mathrm{IVDM}}$ denote the reference results and results from *IVDM*, respectively. In the presented example, the reference values are calculated according the Newmark integration scheme for the structure with modified cross-sections presented in Table 1.

The relative error values of displacements, velocities, and accelerations for the second node (horizontal direction) for a structure with modifications simulated via IVDM + IMVF and for a structure reanalyzed via FEM with modified cross-sections are presented in Fig. 5. The maximal values of errors do not exceed 2×10^{-7}%.

3.5 Sensitivity analysis

An important advantage of the proposed method based on virtual distortions and forces is the availability of precise, analytically obtained gradients, which plays the crucial role in the optimization procedures. Let us demonstrate how to determine gradients of strain and acceleration fields with respect to the cross-sectional areas. The first step is to differentiate the formula (26):

$$\frac{\partial \varepsilon_i(t)}{\partial \hat{A}_l} = \sum_{\tau<t} D_{ij}^{\varepsilon}(t+1-\tau)\frac{\partial \varepsilon_j^0(\tau)}{\partial \hat{A}_l} + \sum_{\tau<t} B_{iM}^{p}(t+1-\tau)\frac{\partial p_M^{0M}(\tau)}{\partial \hat{A}_l}. \tag{35}$$

The sensitivity of the distortion field $\frac{\partial \varepsilon_j^0(\tau)}{\partial \hat{A}_l}$ with respect to cross-sectional area is being determined by differentiation of formula (9), while the sensitivity of the virtual forces is obtained by differentiation of formula (15):

$$\frac{\partial \varepsilon_i^0(t)}{\partial \hat{A}_l} = -\frac{\partial \mu_i}{\partial \hat{A}_l}\varepsilon_i(t) + (1-\mu_i)\frac{\partial \varepsilon_i(t)}{\partial \hat{A}_l}. \tag{36}$$

The gradient of the strain field with respect to the cross-sectional area $\frac{\partial \varepsilon_i(t)}{\partial \hat{A}_l}$ includes also the component of sensitivity of the *virtual distortions* $\frac{\partial \varepsilon_i^0(t)}{\partial \hat{A}_l}$ in a given time instant t:

$$\frac{\partial \varepsilon_i(t)}{\partial \hat{A}_l} = \frac{\partial \varepsilon_i^{\neq t}(t)}{\partial \hat{A}_l} + D_{ij}^{\varepsilon}(1)\frac{\partial \varepsilon_j^0(t)}{\partial \hat{A}_l} + D_{iM}^{p}(1)\frac{\partial p_M^0(t)}{\partial \hat{A}_l} \tag{37}$$

Table 1 Modification of cross-sections

Elem. no.	μ^A	$\hat{A}$ (mm^2)
1	1.2	120
2	0.8	80
3	0.1	10
4	1.2	120
5	0.2	20

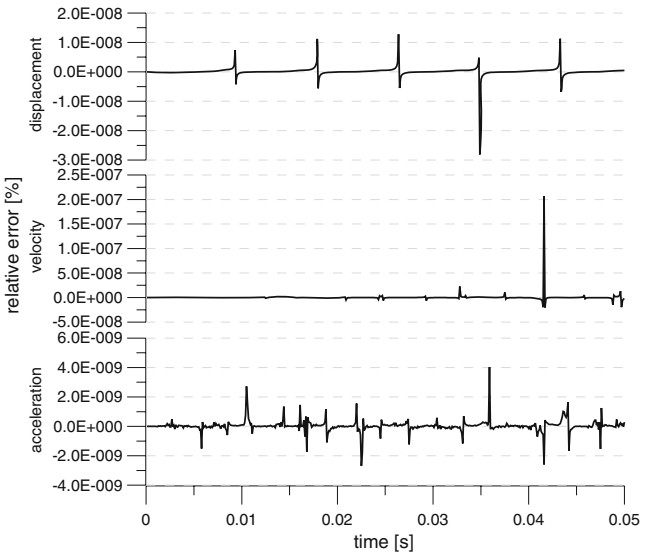

Fig. 5 Relative difference of displacements, velocities, and accelerations for the second node in horizontal direction

where $\frac{\partial \varepsilon_i^{\neq t}(t)}{\partial \hat{A}_l}$ is the sensitivity of the strain field with respect to cross-sections and it does not include the sensitivity of virtual fields for a given time instant t:

$$\frac{\partial \varepsilon_i^{\neq t}(t)}{\partial \hat{A}_l} = \sum_{\tau=1}^{t-1} D_{ij}^{\varepsilon}(t-\tau)\frac{\partial \varepsilon_j^0(\tau)}{\partial \hat{A}_l} + \sum_{\tau=1}^{t-1} D_{iM}^{p}(t-\tau)\frac{\partial p_M^0(\tau)}{\partial \hat{A}_l}. \tag{38}$$

After substitutions and rearrangements are done, we obtain:

$$\left[\delta_{ij} - (1-\mu_{\underline{i}}^{\mathrm{A}})D_{\underline{i}j}^{\varepsilon}(1)\right]\frac{\partial \varepsilon_j^0(t)}{\partial \hat{A}_l} - (1-\mu_{\underline{i}}^{\mathrm{A}})D_{\underline{i}M}^{P}(1)\frac{\partial p_M^0(t)}{\partial \hat{A}_l} = (1-\mu_i)\frac{\partial \varepsilon_i^{\neq t}(t)}{\partial \hat{A}_l} - \frac{\partial \mu_i}{\partial \hat{A}_l}\varepsilon_i(t). \tag{39}$$

On the other hand, the gradient of virtual forces with respect to cross-sections is obtained in the form:

$$\frac{\partial p_N^0(t)}{\partial \hat{A}_l} = -\frac{\partial \Delta M_{NM}}{\partial \hat{A}_l}\ddot{u}_M(t) - \Delta M_{NM}\frac{\partial \ddot{u}_M(t)}{\partial \hat{A}_l}. \tag{40}$$

Similar to formula (37), the sensitivity of the acceleration field with respect to cross-sections should be expressed via components dependent on virtual fields for a given time instant t in the following form:

$$\frac{\partial \ddot{u}_N(t)}{\partial \hat{A}_l} = \frac{\partial \ddot{u}_N^{\neq t}(t)}{\partial \hat{A}_l} + \ddot{B}_{Nj}^{\varepsilon}(1)\frac{\partial \varepsilon_j^0(t)}{\partial \hat{A}_l} + \ddot{B}_{NM}^{p}(1)\frac{\partial p_M^0(t)}{\partial \hat{A}_l}. \tag{41}$$

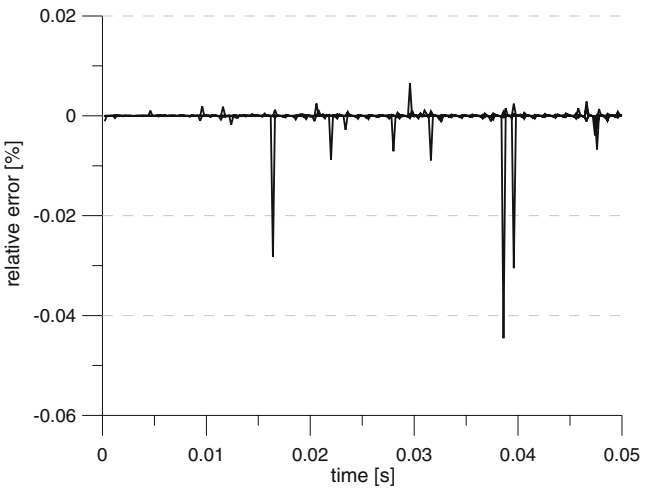

Fig. 6 The relative difference of strain gradients $\frac{\partial \varepsilon_i(t)}{\partial \hat{A}_4}$ computed with VDM and FDM for all elements

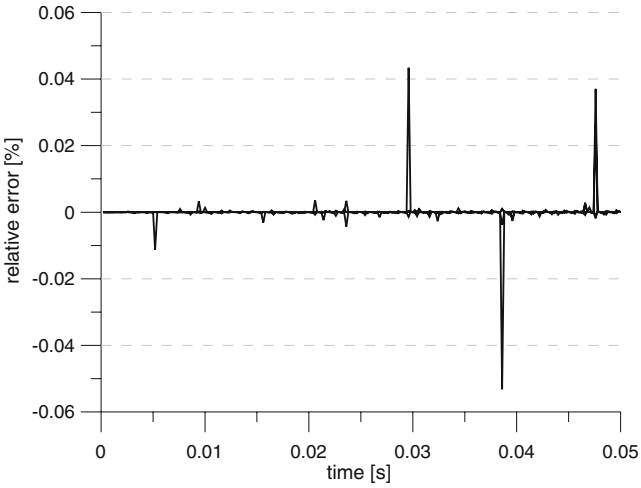

Fig. 7 The relative difference of acceleration gradients $\frac{\partial \ddot{u}_N(t)}{\partial \hat{A}_2}$ computed with VDM and FDM for all degrees of freedom

Substituting (41) to (40) and rearranging the formula, we obtain the second relation necessary for calculation of the resultant virtual field gradients:

$$\Delta M_{NM}\ddot{B}_{Nj}^{\varepsilon}(1)\frac{\partial \varepsilon_j^0(t)}{\partial \hat{A}_l} + \left[\delta_{NM} + \Delta M_{NK}\ddot{B}_{KM}^{p}(1)\right]\cdot\frac{\partial p_M^0(t)}{\partial \hat{A}_l} = -\frac{\partial \Delta M_{NM}}{\partial \hat{A}_l}\ddot{u}_M(t) - \Delta M_{NM}\frac{\partial \ddot{u}_M^{\neq t}(t)}{\partial \hat{A}_l}. \tag{42}$$

The final set of equations is similar to the set modeling of structural cross-section modifications. The principal matrix of (32) is identical. It is time independent, and there is no need for its reformulation during the computation process:

$$\begin{bmatrix} \left[\delta_{ij} - (1-\mu_{\underline{i}}^{\mathrm{A}})D_{\underline{i}j}^{\varepsilon}(1)\right] & (1-\mu_{\underline{i}}^{\mathrm{A}})D_{\underline{i}K}^{P}(1) \\ \Delta M_{NM}\ddot{B}_{Mj}^{\varepsilon}(1) & \left[\delta_{NK} + \Delta M_{NM}\ddot{B}_{MK}^{p}(1)\right] \end{bmatrix} \cdot \begin{bmatrix} \frac{\partial \varepsilon_j^0(\tau)}{\partial \hat{A}_l} \\ \frac{\partial p_K^{0M}(\tau)}{\partial \hat{A}_l} \end{bmatrix} = \begin{bmatrix} (1-\mu_i)\frac{\partial \varepsilon_i^{\neq t}(t)}{\partial \hat{A}_l} - \frac{\varepsilon_i(t)}{A_l}\delta_{il} \\ -\frac{\partial \Delta M_{NM}^k}{\partial \hat{A}_l}\ddot{u}_M(t) - \Delta M_{NM}^k\frac{\partial \ddot{u}_M^{\neq t}(t)}{\partial \hat{A}_l} \end{bmatrix}. \tag{43}$$

The relation $\frac{\partial \mu_i(t)}{\partial \hat{A}_l} = \frac{1}{A_l}\delta_{il}$ was applied in the gradient calculations, and the component $\frac{\partial \Delta M_{NM}^k}{\partial \hat{A}_l}$, which appears in the above equation, is described by the formula:

$$\frac{\partial \Delta M_{NM}^k}{\partial \hat{A}_l} = \rho_l l_l \overset{l}{a}{}_{Nr}^{T} M_{rs}^{el} \overset{l}{a}{}_{sM}. \tag{44}$$

The diagrams depicted presents an absolute discrepancy value for gradients (35) and (41) obtained via the finite differences method (FDM) versus gradients analytically determined (VDM-based). The absolute

discrepancy value was calculated for strains in all elements with respect to the cross-sectional area in the fourth element (Fig. 6) and for accelerations in all degrees of freedom with respect to the cross-sectional area in the second element (Fig. 7). The maximal values of discrepancies do not exceed 0.05% for both diagrams. The objective for this comparison was to check if the VDM-based sensitivity algorithm was properly implemented. In more "sensitive" cases, however, analytical results obtained via VDM techniques will be more accurate than those based on FDM. This difference can be crucial for more challenging optimization problems.

4 Optimal remodeling for impact loads

The fast reanalysis technique and possibility of numerically efficient structural modifications, together with an accurate sensitivity analysis, supply us with strong numerical tools to solve various optimization problems. Let us demonstrate these possibilities on the truss–beam structure shown in Fig. 9 exposed to impact loads.

Searching for the best structural remodeling to get the stiffest structure with minimal average deflections under a given impact load, the following objective function has been proposed:

$$f(\hat{A}) = \sum_t \sum_M \left[u_M^d(t) - u_M(\hat{A}, t) \right]^2 \tag{45}$$

where $u_M^d(t)$, $u_M(t)$ denote the postulated and remodeled response, respectively, subject to the following constraints:

$$V = \sum_\alpha A_\alpha l_\alpha \mu_\alpha \le \tilde{V} \tag{46}$$

$$A > 0 \tag{47}$$

$$|\sigma| < \tilde{\sigma} \tag{48}$$

where the index M belongs to the set of degrees of freedom in which the displacements are being minimized, $\tilde{V}$ denotes the volume of material for the initial structural configuration, and $\tilde{\sigma}$ denotes the maximal stress level admissible in structural elements. Note that, by substituting the postulated deflections $u_M^d(t)$ as vanishing, minimization of the objective function (45) means the minimization of the average structural deflection observed in selected locations and in a selected time interval.

To simplify the optimization process, the original problem of optimization (45) with constraints (46), (47), and (48) has been replaced with the problem without constraints. A new objective function f_c (49), which consists of the original function (45) and the penalty function applied when active constrains are exceeded, has been introduced. The quadratic penalty method (Stadnicki 2006; Nocedal and Wright 1999) has been applied to the problem

$$\begin{aligned} f_c(\hat{A}) = f(\hat{A}) &+ c_1 \left(V - \tilde{V} \right)^2 1_{V>\tilde{V}} + c_2 \sum_i \left(\hat{A}_i \right)^2 1_{0>A_i} \\ &+ c_3 \sum_t \sum_i \Big[(\sigma_i(t) + \tilde{\sigma}_i)^2 \, 1_{-\tilde{\sigma}_i > \sigma_i(t)} \\ &+ (\sigma_i(t) - \tilde{\sigma}_i)^2 \, 1_{\tilde{\sigma}_i < \sigma_i(t)} \Big] \end{aligned} \tag{49}$$

where constants c_1, c_2, and c_3 are parameters of penalty. The applied optimization algorithm requires the analytically determined first and the second derivatives of the new objective function f_c:

$$\begin{aligned} \frac{\partial f_c(\hat{A})}{\partial \hat{A}_l} = \frac{\partial}{\partial \hat{A}_l} f(\hat{A}) &+ 2c_1 \left(V - \tilde{V} \right) l_l 1_{V>\tilde{V}} + 2c_2 \hat{A}_l 1_{0>A_l} \\ &+ 2c_3 \sum_t \sum_i \Big[(\sigma_i(t) + \tilde{\sigma}_i) \frac{\partial \sigma_i(t)}{\partial \hat{A}_l} 1_{-\tilde{\sigma}_i > \sigma_i(t)} \\ &+ (\sigma_i(t) - \tilde{\sigma}_i) \frac{\partial \sigma_i(t)}{\partial \hat{A}_l} 1_{\tilde{\sigma}_i < \sigma_i(t)} \Big] \end{aligned} \tag{50}$$

- Derivative of structure response with respect to cross-section modification $\frac{\partial u_k(t)}{\partial \hat{A}_\varphi}$
- Gradient of the objective function $\nabla f_c(\hat{A})$
- Approximate Hessian of the objective function $\tilde{H}(\hat{A})$
- Adaptive selection of optimization increment: repeat
  - Length of optimization increment $\left[\tilde{H}(\hat{A}) + \lambda I \right] \Delta\hat{A} = -\nabla f_c(\hat{A})$
  - Response of structure at new point $\hat{A} + \Delta\hat{A}$, $u_k(\hat{A} + \Delta\hat{A}, t)$ and $f(\hat{A} + \Delta\hat{A})$
  - Predicted improvement of the objective function in new point $\tilde{f}(\hat{A}) - \tilde{f}(\hat{A} + \Delta\hat{A}) = \frac{1}{2} \Delta\hat{A} \left[\lambda I \Delta\hat{A} - \nabla f(\hat{A}) \right]$
  - Improvement parameter of objective function $\rho = \frac{\tilde{f}(\hat{A}) - \tilde{f}(\hat{A} + \Delta\hat{A})}{f(\hat{A}) - f(\hat{A} + \Delta\hat{A})} = \frac{\text{predicted improvement}}{\text{actual improvement}}$
  - If $\rho < \rho_{\min}$, then $\lambda = k\lambda$
  - Otherwise if $\rho > \rho_{\max}$, then $\lambda = \lambda / k$

  Until $\rho \ge 0$

Fig. 8 Single step of the optimization algorithm

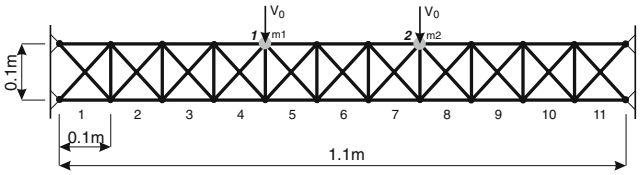

Fig. 9 Two-dimensional truss–beam, initial configuration

$$\frac{\partial^2 f_c(\hat{A})}{\partial \hat{A}_l \partial \hat{A}_k} \approx \frac{\partial^2 f(\hat{A})}{\partial \hat{A}_l \partial \hat{A}_k} + 2c_1 l_l l_k 1_{V>\tilde{V}} + 2c_2 \delta_{lk} 1_{0>A_l} + 2c_3 \sum_t \sum_i \left[\frac{\partial \sigma_i(t)}{\partial \hat{A}_l} \frac{\partial \sigma_i(t)}{\partial \hat{A}_k} 1_{\tilde{\sigma}_i > |\sigma_i(t)|} \right]. \quad (51)$$

Due to the difficulty in the calculation of $\frac{\partial^2 \sigma_i(t)}{\partial \hat{A}_l \partial \hat{A}_k}$, it is assumed to be neglected in (51).

The derivatives of the objective function f are determined by the following relations:

$$\frac{\partial f(\hat{A})}{\partial \hat{A}_l} = -2 \sum_t \sum_M \left[u_M^d(t) - u_M(\hat{A}, t) \right] \times \frac{\partial u_M(\hat{A}, t)}{\partial \hat{A}_l} \quad (52)$$

$$\frac{\partial^2 f(\hat{A})}{\partial \hat{A}_l \partial \hat{A}_m} = 2 \sum_t \sum_M \frac{\partial u_M(\hat{A}, t)}{\partial \hat{A}_l} \frac{\partial u_M(\hat{A}, t)}{\partial \hat{A}_m} - 2 \sum_t \sum_M \left[u_M^d(t) - u_M(\hat{A}, t) \right] \times \frac{\partial^2 u_M(\hat{A}, t)}{\partial \hat{A}_l \partial \hat{A}_m}. \quad (53)$$

Due to complications in the determination of the second derivative of displacement with respect to the cross-section $\frac{\partial^2 u_M(\hat{A},t)}{\partial \hat{A}_l \partial \hat{A}_m}$, the following approximated second derivative will be applied:

$$\frac{\partial^2 f(\hat{A})}{\partial \hat{A}_l \partial \hat{A}_m} \approx 2 \sum_t \sum_M \frac{\partial u_M(\hat{A}, t)}{\partial \hat{A}_l} \frac{\partial u_M(\hat{A}, t)}{\partial \hat{A}_m}. \quad (54)$$

The procedure scheme, based on the Levenberg–Marquardt's algorithm (Nocedal and Wright 1999; Jankowski 2006), presented in Fig. 8, was applied for minimization of the objective function f_c.

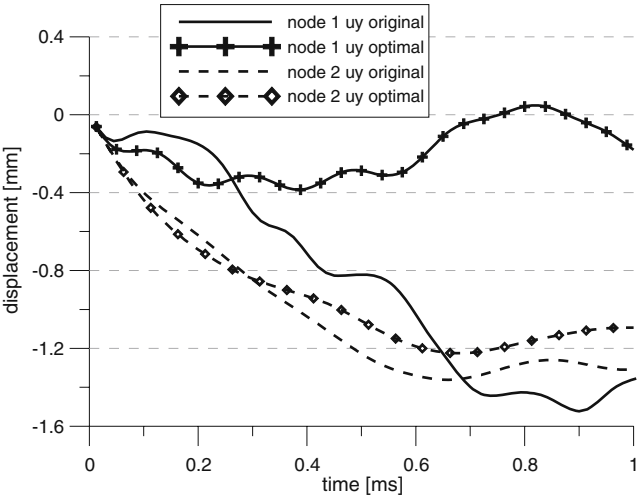

Fig. 11 Response of the original and optimal structure (asymmetric case)

The algorithm should additionally contain the component, which must omit determination of displacements of "liberated" nodes in case when all cross-sections A of elements related with the node become zero. It is easy to implement with virtual methods, because then there is no need to rebuild the stiffness matrix of structure.

The sensitivity of the displacement field with respect to the cross-sectional area, which appears in the algorithm, can be determined by the differentiation of formula (25):

$$\frac{\partial u_j(t)}{\partial \hat{A}_\varphi} = \sum_\xi D_{i\xi}^{\varepsilon}(t+1-\tau) \frac{\partial \varepsilon_\xi^0(\tau)}{\partial \hat{A}_\varphi} + \sum_n D_{in}^{\varepsilon}(t+1-\tau) \frac{\partial p_n^0(\tau)}{\partial \hat{A}_\varphi}. \quad (55)$$

The sensitivity analysis for the distortion field $\frac{\partial \varepsilon_j^0(\tau)}{\partial \hat{A}_l}$ as well as the virtual forces $\frac{\partial p_M^0(\tau)}{\partial \hat{A}_l}$ with respect to the cross-sectional area has already been discussed in the previous section.

The two-dimensional truss–beam, rigidly supported at both ends, was assumed to be the testing model. The structure consists of 11 sections (Fig. 9). The dimen-

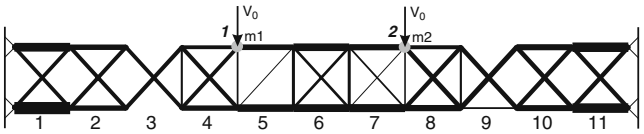

Fig. 10 Optimally remodeled structure with (asymmetric case)

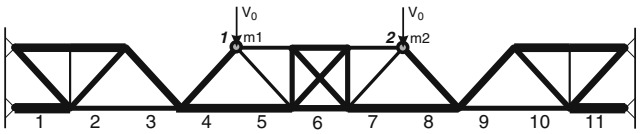

Fig. 12 Optimally remodeled structure (symmetric case)

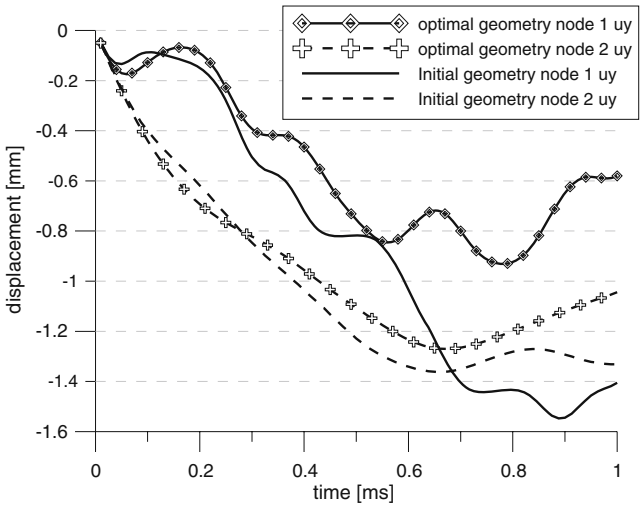

Fig. 13 Response of the original and optimal structure (symmetric case)

sions of each section are 0.1×0.1 m, while its length is 1.1 m. The cross-sectional area of all elements is 110 mm^2. The material used is steel with a Young's modulus of 210 GPa and a density of 7,800 kg/m^3.

The impact load is applied via two masses attached simultaneously to two selected nodes, together with two identical initial velocities (Fig. 9). The mass `m1` imposed to the first node is 0.1 kg, whereas `m2` is 2 kg in the second node. The initial velocity is 5 m/s for both selected nodes. The result of the optimal remodeling solving the problem (45)–(48) is the structure presented in Fig. 10. Selected nodes with minimized deflections are 1 and 2, and the time interval selected for the objective function is $\langle 0, 0.001\ \mathrm{s}\rangle$. Figure 11 demonstrates the

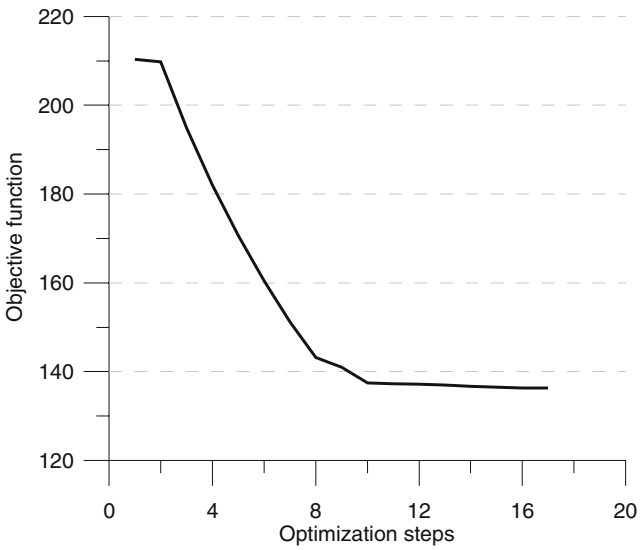

Fig. 14 History of the objective function reduction (symmetric case) for the 30 element construction

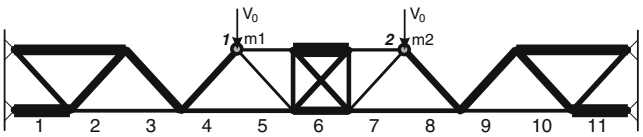

Fig. 15 Optimally remodeled structure (symmetric case) for 26 elements

resultant deflections. The objective function is reduced from 172.24 in the first step to 80.92 for the optimal solution.

Significant mass concentration in selected structural elements is an important side effect of the remodeling process, which will be used in the second part of this paper for effective location of shock absorbers in adaptive versions of the discussed structure.

It is important for the further discussion (adaptive structure discussed in the second part of this paper) to consider the multi-impact-load case. To this end, let us assume that two impact scenarios are possible. The first was just discussed, and the second one differs in the distribution of the impacting masses: mass `m1` $= 0.1$ kg impacting node 2 and `m2` $= 2$ kg impacting node 1. The optimization problem is still based on the algorithm presented in Fig. 8. The difference relates to the $\Delta\hat{A}$ increment, which is being summed and bisected into symmetrical elements:

$$\hat{A}_\alpha + \frac{\left(\Delta\hat{A}_\alpha + \Delta\hat{A}_{\bar{\alpha}}\right)}{2} = \hat{A}_{\bar{\alpha}} + \frac{\left(\Delta\hat{A}_\alpha + \Delta\hat{A}_{\bar{\alpha}}\right)}{2} \qquad (56)$$

where $\bar{\alpha}$ denotes the element symmetrical to the element labeled by α. The structure optimally remodeled for two possible states of impacts is presented in Fig. 12, while further results are shown in Figs. 13 and 14.

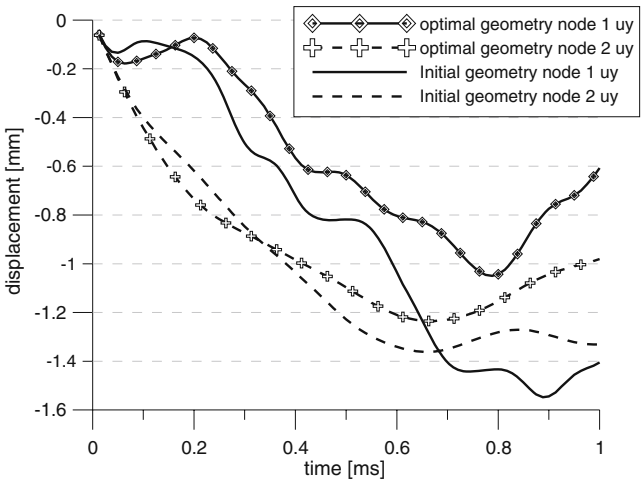

Fig. 16 Response of the original and optimal structure 26 elements (symmetric case)

The optimization algorithm in the current form does not allow eliminating unneeded nodes and replacing two remaining collinear elements with one (local minimum case). Therefore, these modifications are done manually. However, the application of an automatic algorithm for these modifications is also possible. The total number of structural elements has been reduced from 54 (Fig. 9) to 30 (Fig. 10).

The result obtained for the multi-load case is inferior to the previous one (from the objective function viewpoint), but it allows getting important improvement when structural adaptivity will be taken into account in the second part of this paper.

Note that a different solution (Figs. 15 and 16, with the objective function value very close to that obtained above) can be reached by removing the horizontal elements between sections 1 and 2 and 10 and 11 and replacing two upper elements from those sections with one. The cross-sections of the replaced elements have been changed for their mean value. This last 26-element structure will be discussed in the second part of this paper.

5 Conclusions and further steps

The VDM-based techniques for fast structural dynamic reanalysis have been developed in this paper presenting new algorithms for the simulation of structural modifications (coupled modifications of stiffness and mass distribution). Having these algorithms implemented, including the corresponding sensitivity analysis, the problem of optimal remodeling for structures exposed to several possible impact loads has been formulated and solved. The assumed objective function selects, via the gradient based optimization process, the stiffest structure with material concentrated in the overloaded elements. This resulting structural geometry, with modified topology after elimination of several elements, will be a basis for the design of optimally adapting structures with maximum effectiveness of impact load (randomly generated) absorption. The second part of this paper is devoted to the presentation of this concept.

Acknowledgements The authors gratefully acknowledge the financial support by the State Committee for Scientific Research in Poland through the projects IN-MAT (PBZ-KBN-115/T08 2008) and INTEGRA (R10 005 02). Parts of this paper will be used in the coming book "Smart Technologies for Safety Engineering," which will be published by John Wiley and Sons in 2008.

References

Bendsoe MP, Taylor JE (1984) An interpretation for min-max structural design problems including a methods for relaxating constrain. Int J Solids Struct 20(4):301–314

Diaz AR, Bendse MP (1992) Shape optimization of multipurpose structures by homogenization method. Struct Optim 4: 17–22

Diaz AR, Soto CA (1999) Lattice models for crash resistant design and optimization. In: Proc. of 3rd world congress of structural and multidisciplinary optimization, Buffalo, New York, USA, 17–21 May 1999

El-Bkaily MA, Bakkar JY, Mahmood HF, Wheatley DG (1993) On the front end design of automotive vehicle crashworthiness. Crashworthiness and occupant protection in transport systems, AMD-vol. 169, New York ASME, p 331318

Holnicki-Szulc J, Gierlinski T (1995) J. structural analysis, design and control by the virtual distortion method. Wiley

Holnicki-Szulc J, Knap L (1999) Optimal design of adaptive structures for the best crashworthiness. In: Proc. of 3rd world congress of structural and multidisciplinary optimization, Buffalo, New York, USA, 17–21 May 1999

Holnicki J, Knap L (2004) Adaptive crashworthiness concept. Int J Impact Eng 30(6):639–663, July

Ignatovich CL, Diaz AR (2002) Lattices, tuning and space mapping in approximations of structures under impact loads. Third ISSMO/AIAA Internet Conference, October 2002

Ignatovich CL, Diaz AR, Soto CA (2000) On improving the accuracy of lattice models in crashworthiness analysis. In: Proc. of DETC00 ASME design engineering technical conference, Baltimore, Maryland, 10–13 September 2000

Jankowski L (2006) Programming, numerics and optimisation, SMART-TECH expert course, educational materials, http://smart.ippt.gov.pl/

Kamal MM (1970) Analysis and simulation of vehicle-to-barrier impact. SAE Tran. 79, SAE Paper no. 700414

Kamal MM, Wolf Jr JA (1982) Modern automotive structural analysis. Crashworthiness and occupant protection in transport systems, AMD-vol. 169. Van Nostrand Reinhold, New York

Kikuchi N, Bendse MP (1992) Generating optimal topologies in structural design using homogenization method. Comput Methods Appl Mech Eng 71:197–224

Kikuchi N, Yuge K, Iwai N (1998) Topology optimization algorithm for plates and shells subjected to plastic deformations. In: Proc. ASME design engineering technical conference, 1998

Kim CH, Mijar AR, Arora JS (2001) Development of simplified models for design and optimization of automotive structures for crashworthiness. Struct Multidisc Optim 22, Springer

Kolakowski P, Wiklo M, Holnicki-Szulc J (2007) The virtual distortion method (VDM)—a versatile reanalysis tool for structures and systems. Int J Struct Optim doi:10.1007/s00158-007-0158-7

Marzec Z, Holnicki-Szulc J (1999) Adaptive barriers with maximal impact energy absorption. In: Proc. of 3rd world congress of structural and multidisciplinary optimization, Buffalo, New York, USA, 17–21 May 1999

Maute K, Schwartz S, Ramm E, (1998) Adaptive topology optimization of elastoplastic structures. Struct Optim 15(2): 81–91

Mayer RR, Kikuchi N, Scot RA (1996) Application of topological optimization techniques to structural crashworthiness. Int J Numer Methods Eng 39:1383–1403

Mijar AR, Arora JS, Kim CH (1999) Simplified models for automotive crash simulation and design optimization. In: Proc. of 3rd world congress of structural and multidisciplinary optimization, Buffalo, New York, USA, 17–21 May 1999

Nocedal J, Wright SJ (1999) Numerical optimization. Springer

Pedersen CBW (2002a) Topology optimization of 2D-frame structures with path-dependent response. Int J Numer Methods Eng 57(10):1471–1501

Pedersen CBW (2002b) Topology optimization for crashworthiness of frame structures. ICrash Society of Automotive Engineering, Australia, February

Pedersen CBW (2002c) On Topology design of frame structures for crashworthiness. PhD Thesis, Technical University of Denmark, 4

Sekua K, Mikulowski G, Holnicki J (2006) Real time dynamic mass identification. In: Structural health monitoring—third European workshop, Grenada, Spain, 5–6 July 2006

Soto CA (2002) Application of structural topology optimization in the automotive industry: past, present and future. In: Proc. of 5th world congress of computational mechanics, Vienna, Austria, 7–12 July 2002

Song JO, Ni CM (1986) Computer-aided design analysis methods for vehicle structural crashworthiness. In: Proc. symp. on vehicle crashworthiness including impact biomechanics, AMD-vol.79, ASME, New York, p 125139

Stadnicki J (2006) Theory and practice of solving optimization problems with technical examples, WNT (in Polish)

Steinhauser R, Kreisselmeier G (1979) Systematic control design by optimizing a vector performance index. In: IFAC, Symp. computer aided design of control systems, Zurich, Switzerland

Tvergaard V (1975) On the optimum shape of a fillet. In: Sawczuk A, Mroz Z (eds) Proc. IUTAM Warsaw 1973. Optimization in structural design, Spriger, Berlin, pp 181–195

Wang JT, Bennet JA, Lust RV (1991) Optimal design strategies in crashworthiness and occupant protection. Crashworthiness and occupant protection in transport systems, AMD-vol.126 New York, ASME

Zieliski TG (2004) Impulse virtual distortion method and applications to modelling and identification of structural damages. PhD Thesis, Institute of Fundamental Technological Research, IPPT- PAN, 3 (in Polish)